Ecological Engineering 112 (2018) 105–115

Contents lists available at ScienceDirect

Ecological Engineering

journal homepage: www.elsevier.com/locate/ecoleng

The influence of hyporheic upwelling fluxes on inorganic nitrogen concentrations in the pore water of the Weihe River

Weize Wang[a], Jinxi Song[a,b,*], Guotao Zhang[c,d], Qi Liu[a], Weiqiang Guo[a], Bin Tang[a], Dandong Cheng[b,d], Yan Zhang[a]

[a] Shaanxi Key Laboratory of Earth Surface System and Environmental Carrying Capacity, College of Urban and Environmental Sciences, Northwest University, Xi'an 710127, China
[b] State Key Laboratory of Soil Erosion and Dryland Farming on the Loess Plateau, Institute of Soil and Water Conservation, Chinese Academy of Sciences, Yangling 712100, China
[c] Key Laboratory of Mountain Hazards and Earth Surface Process, Institute of Mountain Hazards and Environment, Chinese Academy of Sciences, Chengdu 610041, China
[d] University of Chinese Academy of Sciences, Beijing 100049, China

ARTICLE INFO

Keywords:
Hyporheic zone
Nitrogen
Pore water
The Weihe River
Upwelling fluxes

ABSTRACT

Hyporheic zone is an important region of nitrogen removal in river systems. Hyporheic exchange generally leads to heterogeneous redox environments, which are conducive to nitrogen transformation. This study seeks to determine the influence of hyporheic upwelling fluxes on inorganic nitrogen (NH_4^+, NO_3^-, and NO_2^-) concentrations in the sediment pore water of the Weihe River, China. The patterns and magnitudes of hyporheic water exchange on 12 August 2016 were derived by a one-dimensional heat transport model, and inorganic nitrogen concentrations in the pore water, surface water, and groundwater were obtained. The results indicated that hyporheic water exchange was characterized by upwelling at each point during the test period. Moreover, NH_4^+ dominated the hyporheic zone from 0 to 45 cm, likely due to organic nitrogen mineralization. Additionally, a non-linear relationship was observed between NH_4^+ concentrations and upwelling fluxes. This relationship was derived by analyzing the effect of upwelling on biogeochemical activity and nitrogen transformation. Notably, increasing upwelling fluxes less than 400 mm/d resulted in high NH_4^+ concentrations, whereas fluxes exceeding 400 mm/d led to low NH_4^+ concentrations. Overall, the variations in inorganic nitrogen associated with hyporheic water exchange are of great importance for controlling nitrogen pollution and maintaining sustainable health in river systems.

1. Introduction

The global production and application of fertilizers and fossil fuels are of great concern due to their significant effects on human health and the natural environment (Aslyng, 1984; Rankinen et al., 2014). The amount of fixed nitrogen has doubled over the past several decades because of the influence of human activities (Cai et al., 2007). Stream systems are vital to terrestrial transport and the transformation of dissolved inorganic nitrogen (including NH_4^+, NO_3^- and NO_2^-), which can lead to increase in nitrogen loading in surface water, the hyporheic zone, and groundwater (Bardini et al., 2012), especially in arid and semiarid regions (Wang et al., 2008; Wang et al., 2013; Zhang et al., 2014). Many ecological and environmental problems, such as algae blooms, eutrophication, and the extinction of aquatic species, can be caused by high concentrations of inorganic nitrogen in surface waters and the hyporheic zone (Wang et al., 2016; Xue et al., 2016).

The hyporheic zone is the location in the streambed bordered by surface water and groundwater, thus, it is the saturated zone, or kinematic zonation, that connects the stream and groundwater systems (Zarnetske et al., 2012). This zone influences and regulates the biological transformation of inorganic nitrogen (Jones and Holmes, 1996; Boulton et al., 1998; Cardenas, 2015), and it mainly consists of the porous media, which provide suitable living conditions for hyporheic invertebrates and an abundant source of biodiversity (Briggs et al., 2014). In addition, the biological behaviours of hyporheic invertebrates produce inorganic salts, such as NH_4^+ (Ingendahl et al., 2002; Storey et al., 2004). The invertebrates and microorganisms (including bacteria and fungi) in the hyporheic zone are collectively known as biofilm. Thus, the hyporheic zone is an important site of organic matter absorption and inorganic salt release due to its large internal surface area

* Corresponding author at: Shaanxi Key Laboratory of Earth Surface System and Environmental Carrying Capacity, College of Urban and Environmental Sciences, Northwest University, Xi'an 710127, China.
E-mail address: jinxisong@nwu.edu.cn (J. Song).

https://doi.org/10.1016/j.ecoleng.2017.12.012
Received 29 July 2017; Received in revised form 30 October 2017; Accepted 15 December 2017

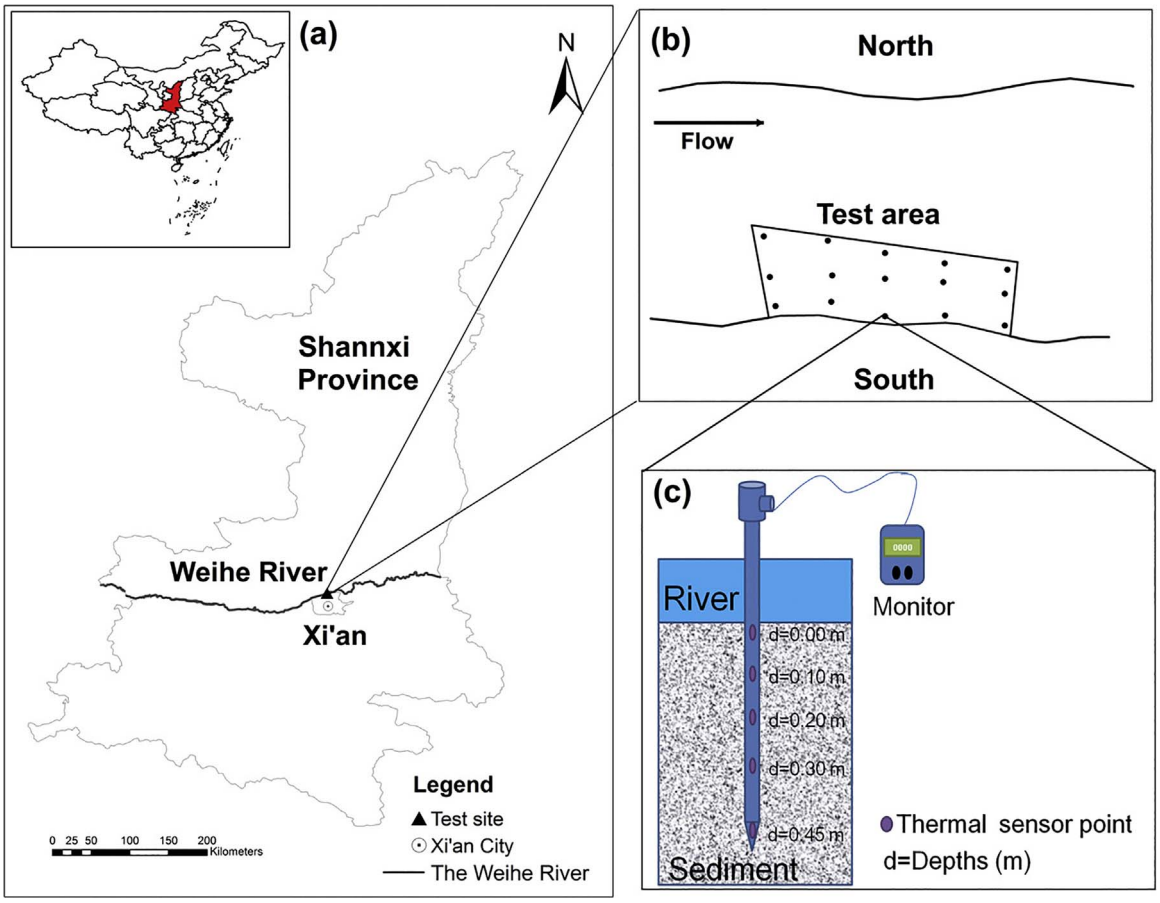

Fig. 1. Map of the study area showing the location of the test site (a), the test points in the study reach (b), and a schematic diagram of the equipment used for temperature measurements in the streambed sediment (c).

(Van Raaphorst and Malschaert, 1996). Moreover, dissolved oxygen (DO) in the hyporheic zone is a primary factor that influences nitrogen transformation and the processes of mineralization, nitrification, and denitrification (Sheibley et al., 2003; Zarnetske et al., 2011; Zarnetske et al., 2012). Organic nitrogen is oxidized by ammonifiers to form NH_4^+ in the process of mineralization, while NH_4^+ is oxidized to NO_2^- and transformed into NO_3^- in the process of nitrification (Stoliker et al., 2016). Both mineralization and nitrification are promoted in aerobic conditions, while denitrification exhibits the opposite trend. Denitrification can facilitate the reduction of NO_3^- to dinitrogen gas, which is an important process or reducing the nitrogen content in aquatic ecosystems (Storey et al., 2004). The dynamics of redox conditions are influenced by the patterns and magnitudes of hyporheic water exchange (Franken et al., 2001), which further influence the variability of solute concentrations in the hyporheic zone, including NH_4^+, NO_3^-, and NO_2^- levels (Briggs et al., 2014). Hyporheic downwelling flow can facilitate the movement of surface waters with high DO concentrations into the sediment, providing abundant DO and organic matter to hyporheic microorganisms (Franken et al., 2001). However, shallow groundwater plays a crucial role in the maintenance and restoration of ecosystems, upwelling flows can facilitate the movement of groundwater with low oxygen levels into the sediment, creating a low-oxygen environment in the hyporheic zone (Franken et al., 2001). Thus, the downwelling and upwelling flow patterns can further influence the inorganic nitrogen concentrations in the hyporheic zone (Storey et al., 2004). Additionally, the water residence time is affected by the dynamics of hyporheic water exchange, which influence the variability of nitrogen concentrations in sediment pore water (Briggs et al., 2014). Overall, the fate and transport of inorganic nitrogen are spatially and temporally complex, especially in the hyporheic zone.

A number of field studies have focused on the importance of hyporheic water exchange on nitrate transformations in the hyporheic zone (e.g. Hester et al., 2016; Briggs et al., 2014; Stelzer et al., 2011). However, few studies analysed the effect of hyporheic water exchange on inorganic nitrogen concentrations in pore water. Moreover, many river systems are controlled by human beings, such as dams and water transform project, which can cause the fluctuating of hyporheic water exchange flux (Zachara et al., 2016). These systems commonly exist so that stream-groundwater exchange flux is easily influenced by human activities (Liu et al., 2017). Hence, it is important to determinate of the influence of hyporheic water exchange on inorganic nitrogen concentrations in the pore water, which is crucial to estimate stream-groundwater interaction as well as being highly effective and beneficial for water quality management.

The patterns and magnitudes of hyporheic water exchange can be measured by several methods, including head piezometers (Nowinski et al., 2011), seepage metres (Zhu et al., 2015), differential discharge gauging (Lowry et al., 2007), thermal methods (Hatch et al., 2006), and other methods (Wei et al., 2012). Hatch et al. (2006) noted that heat tracers can be effectively used to determine the patterns and magnitudes of hyporheic water exchange in rivers at various spatial scales. Recently, heat has been increasingly used as a natural tracer to evaluate and quantify hyporheic water exchange (Anderson, 2005; Arriaga and Leap, 2006; Cranswick et al., 2014; Briggs et al., 2016). In addition, the methods of measuring temperature data are convenient and relatively inexpensive. Therefore, heat transport has been increasingly applied to evaluate hyporheic water exchange in different scenarios and simulations (Boano et al., 2014). Stallman (1965) evaluated the temporal and spatial distributions of water exchange at various scales using a one-

dimensional heat transport model (Anderson, 2005). Based on the steady-state thermal assumption, a one-dimensional steady-state heat model was proposed by Bredehoeft and Papaopulos (1965) and further confirmed by Anibas et al. (2009). This model can be used to determine the patterns and magnitudes of hyporheic water exchange at various temporal and spatial scales.

The objectives of this study are (1) to determine the spatial variability in the magnitudes and patterns of hyporheic water exchange at a test site, (2) to investigate the spatial distributions of solute concentrations (NH_4^+, NO_3^-, and NO_2^-) in sediment pore water, and (3) to further explore the effects of hyporheic water exchange on inorganic nitrogen concentrations in sediment pore water.

2. Materials and methods

2.1. Study area

The study was conducted in the Weihe River, the largest tributary of the Yellow River (Fig. 1). The Weihe River originates in the Niaoshu Mountains in Weiyuan County, Ganshu Province, and flows through Ganshu, Ningxia, and Shaanxi Provinces, with a total length of approximately 818 km. In addition, the drainage area of the Weihe River Basin is approximately $1.34 \times 105\,km^2$, ranging from 104°00′28″ E to 108°56′17″ E and from 34°20′57″ N to 34°23′17″ N. The elevation of the river ranges from 325 to 3485 m above sea level, which is a warm, semi-humid continental monsoon climate zone. The annual mean temperature and rainfall range from 7.8–13.5 °C and 558–750 mm, respectively (increasing from north to south). The weather is hot and rainy in summer and cold and dry in winter. Precipitation varies seasonally, with the majority of floods occurring between July and October. In addition, the river basin is mostly covered with loose loess grains that can cause serious siltation in the river channel (Zhang et al., 2017).

The alluvial plain of the Weihe River is a traditional agricultural region, but it has become a typical industrial and residential region due to rapid economic development (Wang et al., 2016). Numerous middle- and large-sized cities exist near the main channel, and many industrial plants, including food factories and paper mills, are located in the downstream reaches of the Weihe River Basin (Xue et al., 2016). In addition, domestic and industrial wastewater input from nearby cities introduces large amounts of nitrogen contaminants into the Weihe River and influence the water quality of the riverine system (Cai et al., 2009; Xue et al., 2016).

The test site is located in Caotan County at the north of Xi'an City, which is in the downstream portion of the Weihe River Basin (Fig. 1a). Field measurements were conducted on 12 August 2016, and a riffle (water depth ranging from 10 to 80 cm) near the south bank of the river was selected for analysis due to equipment limitations. The river width ranges from 135 to 160 m. The materials in the streambed sediment mainly consisted of silt and fine sand. A total of 15 test points at this site were established near the south bank along five transects perpendicular to the flow direction (Fig. 1b). In addition, the distances between each cross section were approximately 10 m. Each transect included 3 test points, and the distance between the points was approximately 5 m.

2.2. Measurements of sediment temperature

This field study was conducted along a 70-m stretch near the south bank of the river in August 2016 (Fig. 1b). The temperatures in the vertical layers of the sediment at the 15 test points were measured using a 2-m long instrument equipped with five thermistors at specific depths (0.00 m, 0.10 m, 0.20 m, 0.30 m, and 0.45 m) (Fig. 1c). The one-dimensional heat transport model required additional temperature data to obtain more accurate hyporheic water-exchange fluxes. Hence, five thermistors at specific depths were installed inside the instrument. The thermistors in different sediment layers began operation after the instrument was inserted into the sediment. A data logger with logging and storage functions was connected to the instrument. This logger was calibrated to ensure that the thermocouples maintained an accuracy of ± 0.05 °C. The measurements ended after a stabilization period of 15 min at each location. Then, the temperature data were further analysed using the one-dimensional heat transport model provided by Bredehoeft and Papaopulos (1965) to obtain the corresponding patterns and magnitudes of hyporheic water exchange.

2.3. Determination of the magnitudes and patterns of hyporheic water exchange

Considering the processes of water exchange in the hyporheic zone, i.e., both convection and conductive transport, the solution developed by Stallman (1965) was applied to determine the magnitudes and patterns of water exchange between surface water and groundwater. Eq. (1) assumes that simultaneous non-steady heat and fluid flow through isotropic, homogeneous, and saturated porous media.

$$\frac{\partial^2 T}{\partial x^2} + \frac{\partial^2 T}{\partial y^2} + \frac{\partial^2 T}{\partial z^2} - \frac{c_f \rho_f}{k}\left[\frac{\partial (v_x T)}{\partial x} + \frac{\partial (v_y T)}{\partial y} + \frac{\partial (v_z T)}{\partial z}\right] = \frac{c_{fs}\rho_{fs}}{k}\frac{\partial T}{\partial t} \tag{1}$$

where

T-temperature at any point at time t (°C)

c_f-specific heat of the fluid ($J\,kg^{-1}\,K^{-1}$)

ρ_f-density of the fluid ($kg\,m^{-3}$)

c_{fs}-specific heat of the solid-fluid complex ($J\,kg^{-1}\,K^{-1}$)

ρ_{fs}-density of the solid-fluid complex ($kg\,m^{-3}$)

k-thermal conductivity of the solid-fluid complex ($J\,s^{-1}\,m^{-1}\,K^{-1}$)

v_x, v_y, v_z-components of the fluid velocity in the x-, y-, and z-directions ($m\,s^{-1}$)

x, y, z-Cartesian coordinates (m)

t-time (s)

When heat and fluid transport are one-dimensional (in the vertical direction) and steady, the differential Eq. (1) can be reduced.

$$c_{fs}\rho_{fs}\left(\frac{\partial T}{\partial t}\right) = k_{fs}\frac{\partial^2 T}{\partial z^2} - c_f \rho_f q\left(\frac{\partial T}{\partial z}\right) \tag{2}$$

Bredehoeft and Papaopulos (1965) analysed the vertical steady anisothermal groundwater flow through a semiconfining bed and found that temperature variations at different depths over time could be ignored. Therefore, an analytical solution was derived for an aquifer system of thickness L.

$$T = T_0 \quad z = 0 \tag{3}$$

$$T = T_L \quad z = L \tag{4}$$

Thus, the general differential Eq. (2) was simplified to Eq. (5) as follows.

$$\frac{T - T_0}{T_L - T_0} = \frac{e^{\beta z/L} - 1}{e^{\beta} - 1} \tag{5}$$

$$\beta = \frac{c_f \rho_f q L}{k_{fs}} \tag{6}$$

where

T-temperature at any depth (°C)

T_0-measured uppermost temperature (°C)

T_L-measured lowermost temperature (°C)

L-vertical distance between the measured uppermost and lowermost temperatures (m)

β is a dimensionless parameter, and it can be positive or negative depending on whether q is downward or upward, respectively. Based on the practical ranges of parameters, Bredehoeft and Papaopulos (1965) provided values of the function $f\ (\beta,\ z/L) = [e^{\wedge}(\beta(z/L)) - 1]/(e^{\wedge}\beta - 1)$ and a series of type curves for different β values.

Table 1
The input parameters of physical properties used in the one-dimensional heat advection-diffusion equation (Eq. (8)) in the study area.

Parameters	Value	Unit
Thermal conductivity, k_{fs}	1.765	$J\,s^{-1}\,m^{-1}\,K^{-1}$
Specific heat capacity of water, c_f	422400	$J\,kg^{-1}\,K^{-1}$
Density of water, ρ_f	1000	$kg\,m^{-3}$
Vertical distance, L	0.45	m

That β was related to the curvature of a temperature-depth profile at several depths ranging from $z = 0$ to $z = L$. The values of β obtained from the type curves matched those based on field data. Boyle and Saleem (1979) used a computer program to obtain the values of β. These temperature data were used to calculate the ratios of $(T - T_0)/(T_L - T_0)$ based on the change in z from 0 to L. Eq. (7) was developed to calculate the sum of squares of the deviations between these ratios, as well as the theoretical values of $f(\beta, z/L)$ for $0 \le z \le L$ and for specified values of T_0, T_L, $L$and β.

$$F(\beta) = \sum_{z=0}^{z=L} \left[\frac{T - T_0}{T_L - T_0} - \frac{e^{\beta z/L} - 1}{e^{\beta} - 1} \right]^2 \tag{7}$$

When the objective function $f(\beta)$ is minimized, the optimum value of β can be determined (Saleem, 1970). In addition, the flux of the hyporheic water exchange (q) can be directly determined as follows.

$$q = \frac{k_{fs}\beta}{c_f \rho_f L} \tag{8}$$

The physical parameters obtained during the test period and used as inputs in Eq. (8) are shown in Table 1. A positive or negative flux (q) indicates downwelling or upwelling flow, respectively.

2.4. Sampling and laboratory analysis

A 160-cm long PVC pipe was inserted into the sediment next to the temperature pipe, and sediment cores were obtained from approximately 45 cm depth beneath the sediment–water interface. The sediment samples were collected via plugging the top of the pipe and inserting it into the riverbed. Then, sediment samples were retained in the pipe when the pipe was removed from the riverbed. The plug can prevent sediments from exiting the bottom of the pipe. Pore water samples were extracted from three depths beneath the sediment interface (0–15 cm, 15–30 cm, and 30–45 cm) to obtain enough pore water every 20 min, in total three pore water samples were obtained at each depth for each test point in an hour, thus creating 1-h average samples. In addition, surface water and groundwater samples were collected at the site. Finally, the samples (including water and sediment samples) were placed in sampling bags or bottles and immediately transported in cold conditions to the laboratory, where they were preserved in a cold environment.

In the laboratory, the pH, electrical conductivity (EC), dissolved oxygen (DO) and oxidation-reduction potential (ORP) of the water samples were measured using a portable multiparameter water quality analyser (HACH HQ40d. Loveland, Colorado, USA). The concentrations of NO_3^-, NH_4^+, NO_2^- in pore water, surface water, and groundwater were determined using an Auto Discrete Analyser (Clever Chem 200, Hamburg, Germany). The average concentrations were calculated at each point. Moreover, the sediment samples were air-dried, and the particle size was categorized into 17 grades using a sieving method. The coarsest particle size was 12 mm, while the finest particle size was 0.075 mm. The particle size was classified into four groups: silt or clay

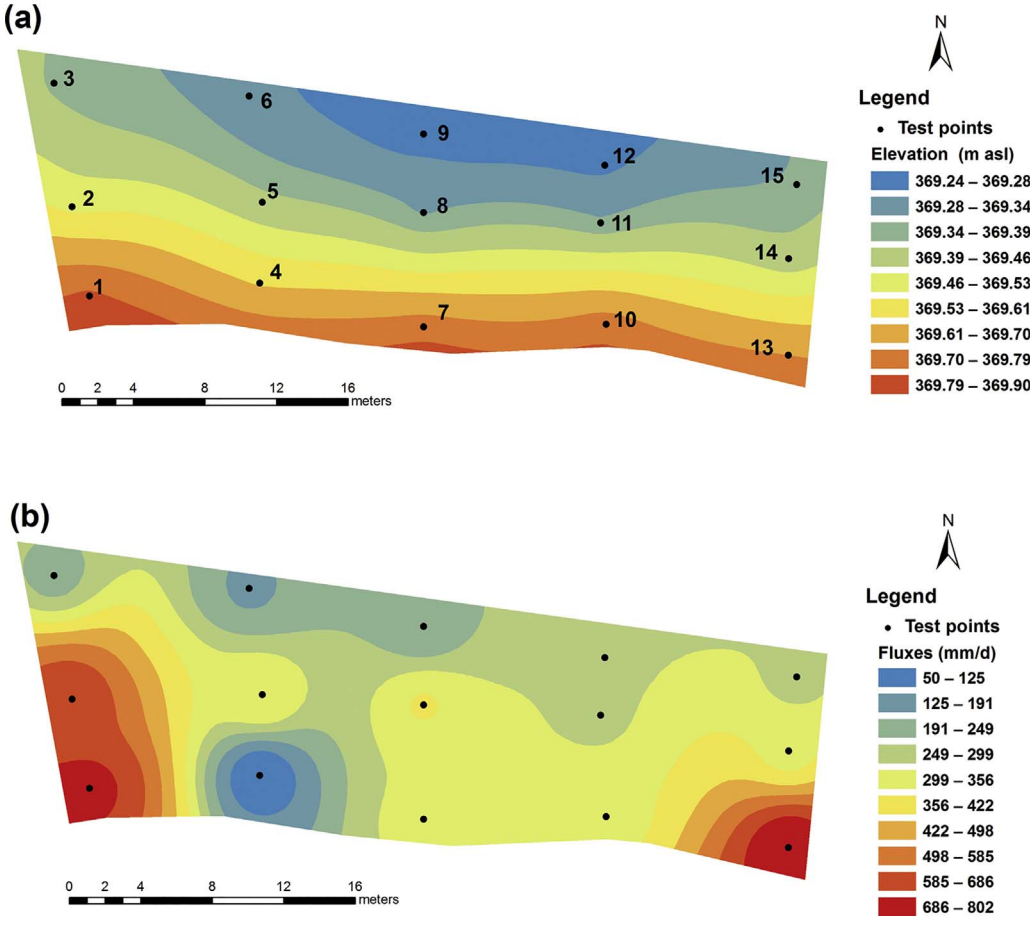

Fig. 2. Streambed elevation above sea level (a) and the spatial distribution of hyporheic water exchange fluxes (b).

less than 0.075 mm, fine sand ranging from 0.075 mm to 0.2 mm, coarse sand ranging from 0.2 mm to 2 mm, and gravel larger than 2 mm. Additionally, the cumulative percentage weights of the sediment samples were calculated to analyse the sediment properties.

2.5. Data analysis

The Kolmogorov-Smirnov test was applied to verify whether the hyporheic upwelling fluxes were normally distributed at a 95% confidence level. Statistical correlation and regression analyses involving the solute concentrations in pore water (NH_4^+, NO_3^-, NO_2^-, and DO) and the hyporheic fluxes were assessed using Pearson's *r* in SPSS 17.0 to determine whether these correlations were significant (P value, the correlation was significant at the 0.05 level).

3. Results and discussion

3.1. Patterns and magnitudes of hyporheic water exchange

The temperatures at five depths beneath the sediment–water interface were measured at 15 test points during the test period. Based on the analyses of the temperature distributions from on-site tests, the patterns and magnitudes of hyporheic water exchange were determined using the one-dimensional heat transport model (Eq. (8)). The fluxes of hyporheic water exchange were obtained at each point, and their spatial variability was illustrated using a visual contour map of the test site (Fig. 2b). The magnitudes of water exchange fluxes at these 15 points was negative, indicating that upwelling hyporheic flow was predominant at the test site during the test period (Fig. 3). The regional groundwater discharged into the river dominated the upwelling flow in the study area. The magnitudes of water exchange at the test site were estimated to range from −50 mm/d to −802 mm/d. Based on the water level data of study area during 8–14 August 2016 (the groundwater level obtained in monitoring well nearby the study site as well as surface water level at the test site) (Fig. 4), it is evident that the groundwater level was higher than surface water level, generally indicating that groundwater discharging into the river at the study site during the test period. Therefore, the relatively high range of upwelling fluxes at the test site was probably driven by groundwater flowing into the river regionally (Song et al., 2017). The mean value was −360 mm/d, reflecting significant spatial variability. Additionally, the Kolmogorov-Smirnov test result of the fluxes fit a normal distribution at the study site ($p = 0.193$). Along channel cross-sections, large upwelling fluxes generally occurred in the vicinity of the south bank, which was shallower than other areas of the cross-sections (Figs. 2 and 3). The streambed elevation reflects the water depth at the test site (Fig. 2a), and a significant negative correlation was observed between the fluxes and water depth (Figs. 2 and 3). Song et al. (2016) suggested that the high pressure head in deep areas likely hindered groundwater discharge through the hyporheic zone into surface water. However, poor correlations were observed at points 4 and 7, and these findings may be related to the sediment grain size. Grain size plays an important role in hydrological processes (Wang et al., 2008; Song et al., 2010). The average cumulative percentage of the sediment grain size by weight was measured at each test point, and the weight percentages of different materials (including gravel, coarse sand, fine sand and clay) were determined at the 15 points (Fig. 5). Additionally, large amounts of clay and less gravel were observed at point 4 and 7 (Fig. 5). Clay layers in the sediment can hinder vertical hyporheic flow into surface water.

3.2. Chemistry of surface water, groundwater, and pore water

The concentrations of NH_4^+, NO_2^-, NO_3^-, and DO, as well as the EC and ORP levels, in surface water, pore water, and groundwater significantly varied (Table 2). At the test site, high NO_3^- concentrations (mean of 6.49 mg/L) and low NH_4^+ concentrations (mean of 1.01 mg/L) were observed in surface waters with high concentrations of DO (mean of 9.6 mg/L), namely, an oxic environment (Table 2). The values of EC and ORP were 559 μs/cm and 65.3 mv, respectively, which indicated that oxidation was occurring in the surface water. Low NO_3^- concentrations (mean of 0.55 mg/L) and high NH_4^+ concentrations (mean of 1.39 mg/L) were obtained in groundwater samples with low concentrations of DO (mean of 4.28 mg/L) (Table 2). The values of EC and ORP were 778 μs/cm and −28.1 mv, respectively, indicating a reduced, low-oxygen environment within the groundwater during the test period. Moreover, the concentrations of NO_2^- were low in surface water and groundwater (Table 2).

Considering the risks to environment and human health, the World Health Organization (WHO) regulates the maximum contaminant levels (MCLs) of NH_4^+ (MCL ≤ 1.0 mg/L in surface water and MCL ≤ 0.2 mg/L in groundwater), NO_2^- (MCL ≤ 0.2 mg/L in surface water and groundwater) and NO_3^- (MCL ≤ 10 mg/L in surface water and groundwater). At the study site, the NO_3^- and NO_2^- concentrations in surface water and groundwater were below the MCLs, while the NH_4^+

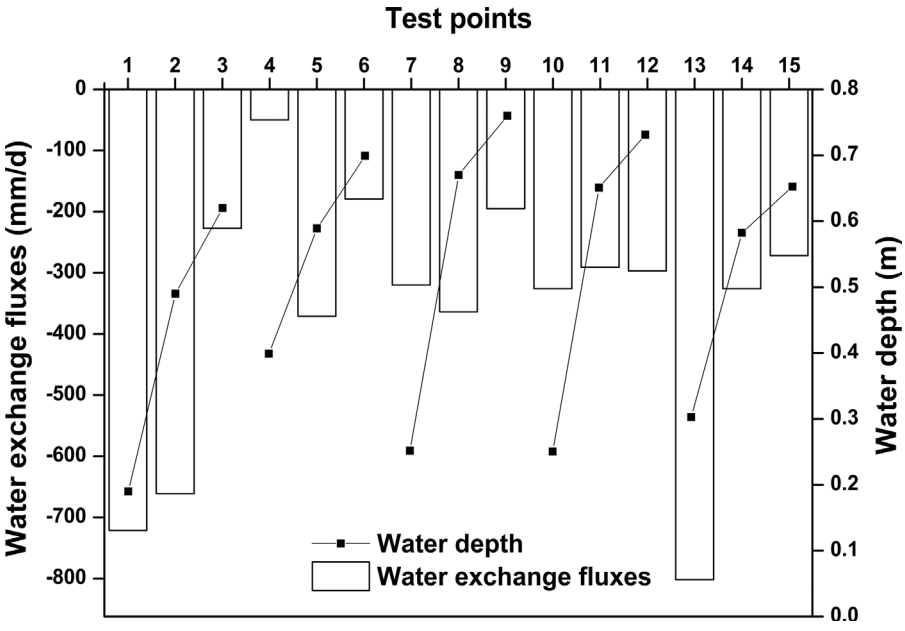

Fig. 3. Patterns and magnitudes of hyporheic water exchange at the test site as well as the water depth at different test points.

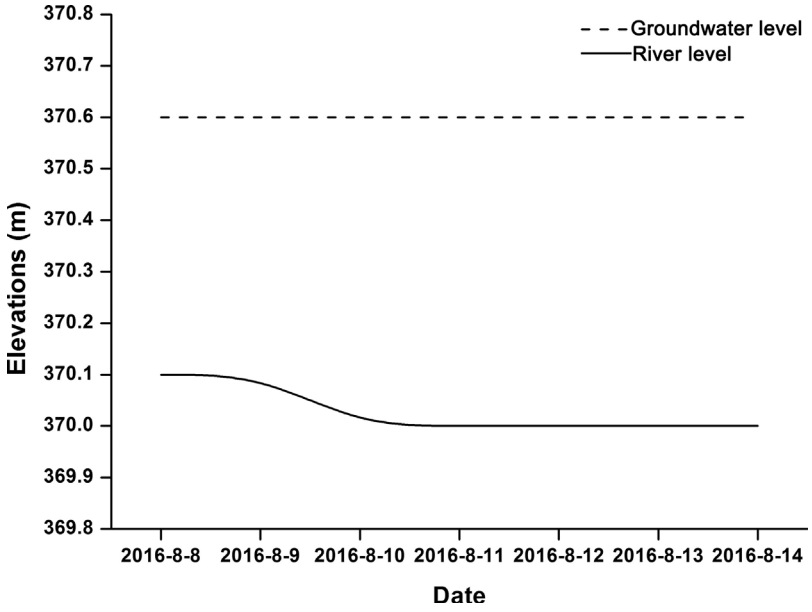

Fig. 4. Groundwater and river levels at the study area from 8 to 14 August 2016.

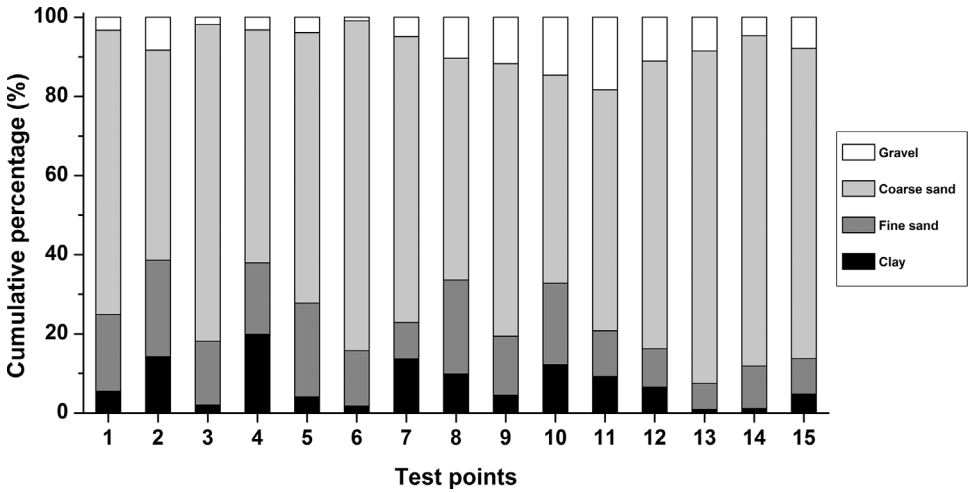

Fig. 5. Average cumulative percentage of the sediment grain size by weight at each test point, including four groups (clay, fine sand, coarse sand, and gravel) based on sediment grain sizes.

Table 2
Mean water chemistry values in pore water, surface water, and groundwater on 12 August 2016.

Parameters	Depths in pore water			Surface water	Groundwater
	0–15 cm	15–30 cm	30–45 cm		
NH_4^+ (mg/L)	13.94	15.64	4.17	1.02	1.39
NO_3^- (mg/L)	1.99	3.10	3.16	6.49	0.55
NO_2^- (mg/L)	0.06	0.04	0.04	0.03	0.01
DO (mg/L)	6.88	6.29	5.62	9.60	4.28
EC (μs/cm)	830.73	759.13	673.27	559	778
ORP (mv)	119.95	118.41	119.07	65.3	−28.1

concentrations in surface water and groundwater exceeded the MCLs during the test period. In addition, a high NH_4^+ concentration existed in groundwater, and the degree of pollution was higher in groundwater than in surface water. Groundwater may have been influenced by nitrogen pollution from the investigated sewage treatment plants in upstream (Ingendahl et al., 2002), meanwhile, irrigated agriculture has a significant impact on groundwater at the study site (Zhang et al., 2004).

The solute concentrations and parameters, including NH_4^+, NO_2^-, NO_3^-, DO, EC, and ORP, in pore water at the three sediment depths beneath the sediment–water interface (0–15 cm, 15–30 cm, and 30–45 cm) were determined at the 15 test points. The concentrations of NO_3^- and NH_4^+ in different pore water layers spatially varied during the test period (Fig. 5a and b). The NO_3^- concentrations in pore water ranged from 0.10 to 9.98 mg/L, while the NH_4^+ concentrations ranged from 0.17 to 32.83 mg/L (Table 2). The mean concentrations of NO_3^- in pore water were 1.99 mg/L, 3.10 mg/L, and 3.16 mg/L at 0–15 cm, 15–30 cm, and 30–45 cm, respectively (Table 2). Additionally, the mean concentrations of NH_4^+ in the three layers were 13.94 mg/L, 15.64 mg/L, and 4.17 mg/L, respectively (Table 2). NH_4^+ dominated the hyporheic zone compared to NO_3^- and NO_2^- at the test site. Duff and Triska (2000) suggested that until sufficient NO_3^- is produced via nitrification, NH_4^+ will dominate rivers. Additionally, significant vertical spatial variability in the solute concentrations of pore water was observed during the test period (Fig. 6). The mean concentration of NO_3^- in pore water increased as the sediment depth increased from 0 to 45 cm, and the NO_3^- concentration increased by 30% in the 30–45 cm layer (Fig. 6b). This increase may be the result of nitrification (Storey et al., 2004). However, the mean concentration of NH_4^+ in pore water exhibited a slight increase in the 15–30 cm layer and then trended to decrease at the lower layers (Fig. 6a). This increase may have been caused by nitrogen mineralization, via which the organic matter in surface water can enter the sediment via deposition and be transformed into NH_4^+ by ammonification (Lafrenière and Lamoureux, 2008).

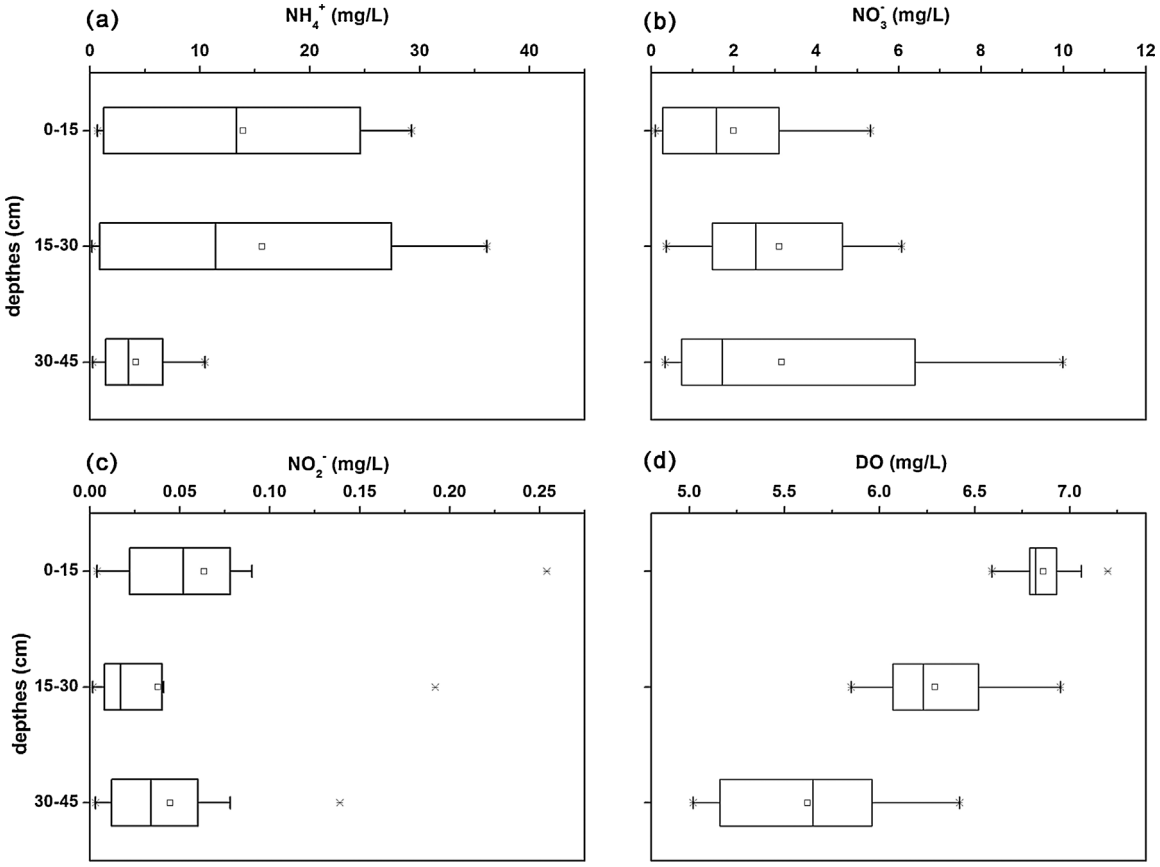

Fig. 6. Box plots of vertical variations in the chemistry of sediment pore water on 12 August 2016, including the NH_4^+ (a), NO_3^- (b), NO_2^- (c), and DO (d) concentrations. The plots consist of median values (vertical lines), interquartile ranges (limits of each box), minimum values, maximum values and outliers (plotted as asterisks).

Moreover, the excreta of invertebrates is a source of at depths of 0–30 cm, where invertebrates are mainly concentrated (Xu et al., 2012).

3.3. Effect of hyporheic water exchange on nitrogen concentrations

Precipitation varies seasonally in the Weihe River Basin, with the majority of floods occurring between July and October. The floods had significant effects on stream ecosystems (Cai et al., 2011). Under high-flow conditions, Gu et al. (2012) suggested that decreased groundwater input to streams and increased surface water residence time promote nitrogen removal in the hyporheic zone. Under minimum-stage conditions, surface water enter into the hyporheic zone is minimal, and the hyporheic water exchange fluxes are not enough to promote abundant groundwater-surface water mixing. Therefore, nitrogen removal is weak in the hyporheic zone (Briody et al., 2016). The primary goal of this study is to investigate the effect of upwelling fluxes on inorganic nitrogen concentrations in the pore water. The field work was conducted on 12 August 2016 to avoid the influence of river flow fluctuation on hyporheic nitrogen concentrations and unstable hyporheic water exchange because both surface water level and groundwater level were approximately steady around the day (Fig. 4). The upwelling fluxes and pore water concentrations of inorganic nitrogen (including NH_4^+, NO_3^-, and NO_2^-) in the 0–45 cm layer were obtained at different test points (Fig. 7a and b) to analyse their spatial distributions in a visual manner. A negative correlation between NO_3^- and NH_4^+ at many points is shown in Fig. 7. This correlation reflects the fate of nitrogen in pore water sediments. NH_4^+ dynamics were an intimate component of NO_3^- cycling (Zarnetske et al., 2012), and NH_4^+ was easily converted to NO_3^- by nitrification under oxic conditions (Lafrenière and Lamoureux, 2008). In this study, the NO_3^- concentrations were relatively low compared with NH_4^+ concentrations in the pore water, and the increase of the NO_3^- with sediment depth was not significant. This result suggests that nitration process is slow at depths of 0–45 cm in the sediment. Additionally, the NO_2^- concentrations in pore water were low at all other test points except point 4 (Fig. 7c). This phenomenon at most points may have been caused by the unstable transformation of NO_2^- into NO_3^- (Schullehner et al., 2017).

Statistical correlation and regression analyses involving the solute concentrations in pore water (NH_4^+, NO_3^-, NO_2^-, and DO) and the hyporheic fluxes were conducted (Fig. 8). Notably, a favourable quadratic polynomial fit was observed between NH_4^+ and the fluxes, indicating a non-linear relationship ($p = 0.018$). For upwelling fluxes less than approximately 400 mm/d, NH_4^+ concentrations exhibited a well-defined increasing trend as the fluxes increased. When the upwelling fluxes reached approximately 400 mm/d, the NH_4^+ concentrations began to decrease with increasing fluxes. These trends can be affected by ammonifiers in the hyporheic zone and the DO level and hyporheic water residence time during the test period (Franken et al., 2001; Ingendahl et al., 2002; Lin et al., 2015). The types and levels of microbial activity were easily determined by the distinct patterns of physical and chemical conditions in the hyporheic zone (Claret and Boulton, 2009). The river water was slightly acidic (pH = 6.37), while groundwater was slightly alkaline (PH = 9.63) at the test site. The large upwelling fluxes (groundwater significantly discharged into the river) during the test period created a comfortable living environment for ammonifiers. An optimum pH of approximately 7.5 was created (Dewes, 1996), and abundant ammonifiers easily mineralized organic nitrogen, which caused NH_4^+ concentrations to increase (Lin et al., 2015). However, when upwelling fluxes are more than approximately 400 mm/d, the DO of pore water can be the primary factor that influences NH_4^+ concentrations and controls the mineralization of organic nitrogen into NH_4^+ (i.e., a redox-sensitive species) (Lin et al., 2015).

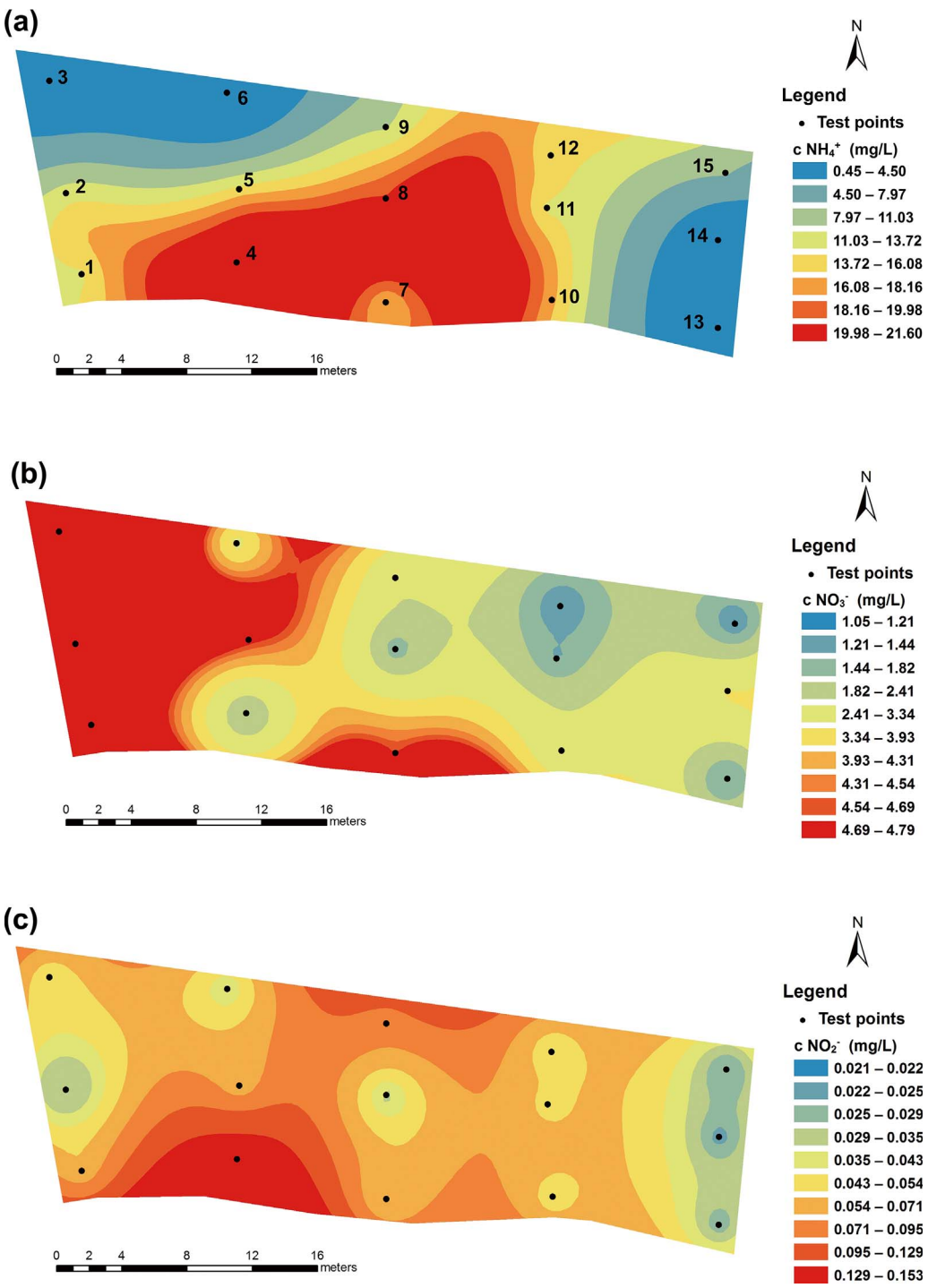

Fig. 7. Spatial distributions of hyporheic NH_4^+ concentrations (a), NO_3^- concentrations (b) and NO_2^- concentrations (c) of pore water in the sediment.

Under the oxic conditions, NH_4^+ easily accumulated in the hyporheic zone due to nitrogen mineralization of dissolved and buried organic material that released NH_4^+ (Storey et al., 2004). Based on the analyses of the ORP and DO concentrations in the hyporheic zone and groundwater (Table 2), groundwater with a low oxygen concentration was readily discharged into the hyporheic zone via upwelling flows. This process decreased DO levels in the hyporheic zone (Fig. 8b). Moreover, a significant negative correlation was observed between the fluxes and DO of pore water in the hyporheic zone at the test site during the test period ($p < 0.01$) (Fig. 8b). This result indicates that the upwelling fluxes decreased the DO concentration of pore water. Upwelling transports low-oxygen groundwater into the hyporheic zone, creating a low-oxygen environment that leads to decreased NH_4^+ concentrations. This finding is opposite that reported by Briggs et al. (2014), who found that hyporheic NH_4^+ concentrations were negatively correlated with DO concentrations in the Little Popo Agie River of the United States. This difference may be associated with the pollution status of each river. Specifically, the study site in the Weihe River is subjected to organic matter pollution, especially from domestic sewage (Li et al., 2013; Wang et al., 2016). The ammonification was dominant in the hyporheic zone from 0 to 45 cm, and most of the DO in the hyporheic zone was consumed via this process, which led to the release of NH_4^+ (Storey et al., 2004).

In addition, the water residence time also played a crucial role in the retention of nutrients and organic matter and influenced the nitrogen cycle processes (Valett et al., 1996). Weak surface water-groundwater

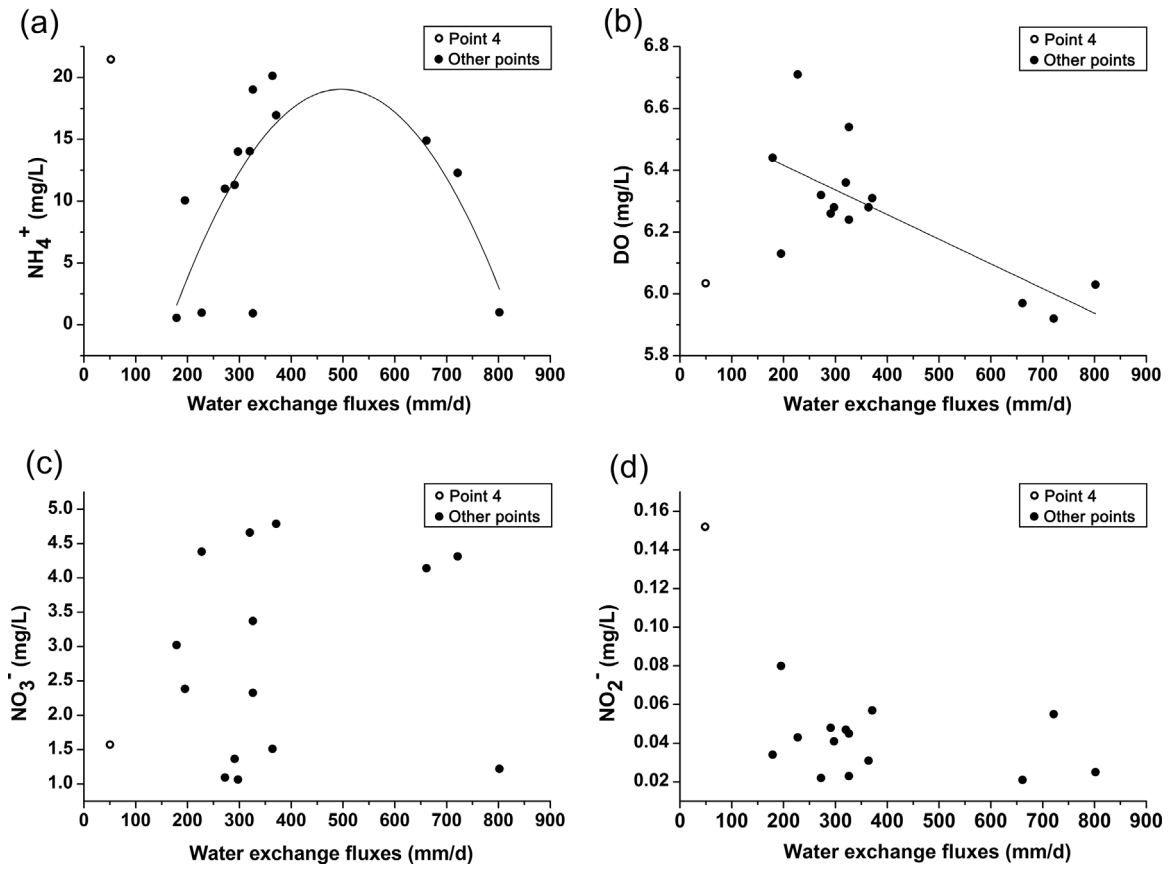

Fig. 8. Relationship between the hyporheic upwelling fluxes and NH_4^+ (a), DO (b), NO_3^- (c), NO_2^- (d) concentrations in the pore water of the sediment during the study period.

exchange indicates a long water residence time (Briggs et al., 2014). In this study, over large water exchange fluxes resulted in short water residence times and low DO concentrations (Storey et al., 2004; Briggs et al., 2014; Heppell et al., 2014). The changes in hydrochemistry and hydrodynamics caused transitions from increase to reduction of NH_4^+ concentration in pore water (Fig. 7a).

However, significant correlations did not exist between upwelling fluxes and NO_3^- or NO_2^- concentrations (Fig. 8c and d). High concentrations of NO_3^- were generally observed in surface water compared to those in pore water (Table 2). In addition, the NO_3^- in surface water can potentially influence the NO_3^- concentration in pore water in the hyporheic zone, as dynamic hyporheic water exchange occurred. Moreover, low NO_2^- concentrations were observed at the test site, except at point 4, where the minimum upwelling flux was observed (−50 mm/d) (Figs. 2b and 7c). In addition, the weak water exchange reflected a long water residence time in the hyporheic zone, indicating that hyporheic microorganisms had more time to mineralize organic nitrogen and consume DO in the hyporheic zone (Briggs et al., 2014). High concentrations of NH_4^+ and NO_2^- and a low NO_3^- concentration were observed at point 4 under low DO conditions (Fig. 8). These results suggest dissimilatory nitrate reduction to ammonium (DNRA) was occurred at point 4 (Cheng et al., 2016). Cheng et al. (2016) found that the DNRA measured at some study points contributed to 50% of nitrate reduction. Additionally, the largest concentration of NH_4^+ in pore water was observed at point 4 (21.59 mg/L), which had the most clay (Figs. 7a, 5). This clay readily hinders the upwelling to generate the interception of NH_4^+ in pore water (Van Raaphorst and Malschaert, 1996).

4. Conclusions

In this study, the spatial variability of hyporheic water exchange and inorganic nitrogen concentrations in the pore water at Xi'an section of the Weihe River, China, were analysed and discussed. The solute concentrations in pore water (NH_4^+, NO_3^-, NO_2^-, and DO) and the hyporheic flux data were collected in the field on 12 August 2016.

The study results are as follows:

(1) Hyporheic water exchange was characterized by upwelling flows at all test points, and the fluxes ranged from −50 mm/d to −802 mm/d during the test period. The low fluxes occurred at deep test points, and the grain size played a crucial role in water exchange processes. Notably, more clay contents led to low water exchange fluxes.
(2) NH_4^+ dominates the hyporheic zone from 0 to 45 cm, and large spatial variations in nitrogen concentrations, including NH_4^+ and NO_3^-, were observed. The NH_4^+ concentrations decreased and NO_3^- concentrations increased with sediment depth.
(3) A non-linear relationship between NH_4^+ concentrations and upwelling fluxes was found in the hyporheic zone. When the upwelling flux was less than approximately 400 mm/d, the NH_4^+ concentrations increased with the flux. This trend may be related to the pH, which slightly increased as the upwelling flux increased. This process created a living environment with a pH suitable for ammonifiers. The abundant ammonifiers mineralized organic nitrogen and increased the NH_4^+ concentrations. Additionally, the water residence time had a significant effect on nitrogen transformation when the upwelling flux was greater than approximately 400 mm/d. A short water residence time weaken organic nitrogen mineralization, which led to low concentrations of NH_4^+. Moreover, decreases in DO concentrations also led to decrease in NH_4^+ concentrations.

This study investigated the spatial distribution of inorganic nitrogen

in pore water and determined the interaction of groundwater and surface water in the Weihe River, further analysed the influence of hyporheic upwelling fluxes on inorganic nitrogen concentrations in the pore water. The results that we obtain from this study can provide important information to adjust hyporheic water exchange by hydrologic controls for nitrogen removal in hyporheic zone as well as being efficient for water resource management. However, this study only illustrates the vertical characteristics of hyporheic water exchange. In future studies, the water exchange in other directions and additional hydrological parameters should be considered. To better understand the effects of hyporheic water exchange on inorganic nitrogen concentrations in the pore water of the Weihe River, further the abundance and diversity of microorganisms must be assessed.

Acknowledgements

This study was jointly supported by the National Natural Science Foundation of China (Grant Nos. 51379175, 51679200 and 41601017), Program for Key Science and Technology Innovation Team in Shaanxi Province (Grant No. 2014KCT-27) and the Hundred Talents Project of the Chinese Academy of Sciences (Grant No. A315021406). In particular, we are grateful to the editor and two anonymous reviewers for providing numerous comments and suggestions, which helped improve this manuscript.

References

Anderson, M.P., 2005. Heat as a ground water tracer. Groundwater 43, 951–968. http://dx.doi.org/10.1111/j.1745-6584.2005.00052.x.

Anibas, C., Fleckenstein, J.H., Volze, N., Buis, K., Verhoeven, R., Meire, P., Batelaan, O., 2009. Transient or steady-state? Using vertical temperature profiles to quantify groundwater–surface water exchange. Hydrol. Processes 23, 2165–2177. http://dx.doi.org/10.1002/hyp.7289.

Arriaga, M.A., Leap, D.I., 2006. Using solver to determine vertical groundwater velocities by temperature variations, Purdue University, Indiana, USA. Hydrol. J. 14, 253–263. http://dx.doi.org/10.1007/s10040-004-0381-x.

Aslyng, H.C., 1984. Nitrogen balance in fertilizer application and plant production. In: (Nyborg, Denmark, August – 1984). Paper Presented at the Nordic Hydrological Conference 15. pp. 169–176.

Bardini, L., Boano, F., Cardenas, M., Revelli, R., Ridolfi, L., 2012. Nutrient cycling in bedform induced hyporheic zones. Geochim. Cosmochim. Acta 84, 47–61. http://dx.doi.org/10.1016/j.gca.2012.01.025.

Boano, F., Harvey, J.W., Marion, A., Packman, A.I., Revelli, R., Ridolfi, L., Wörman, A., 2014. Hyporheic flow and transport processes: mechanisms, models, and biogeochemical implications. Rev. Geophys. 52, 603–679. http://dx.doi.org/10.1002/2012RG000417.

Boulton, A.J., Findlay, S., Marmonier, P., Stanley, E.H., Valett, H.M., 1998. The functional significance of the hyporheic zone in streams and rivers. Annu. Rev. Ecol. Syst. 29, 59–81.

Boyle, J.M., Saleem, Z., 1979. Determination of recharge rates using temperature-depth profiles in wells. Water Resour. Res. 15, 1616–1622.

Bredehoeft, J., Papaopulos, I., 1965. Rates of vertical groundwater movement estimated from the Earth's thermal profile. Water Resour. Res. 1, 325–328.

Briggs, M.A., Lautz, L.K., Hare, D.K., 2014. Residence time control on hot moments of net nitrate production and uptake in the hyporheic zone. Hydrol. Processes 28, 3741–3751. http://dx.doi.org/10.1002/hyp.9921.

Briggs, M.A., Buckley, S.F., Bagtzoglou, A.C., Werkema, D.D., Lane, J.W., 2016. Actively heated high-resolution fiber-optic-distributed temperature sensing to quantify streambed flow dynamics in zones of strong groundwater upwelling. Water Resour. Res. 52, 5179–5194. http://dx.doi.org/10.1002/2015WR018219.

Briody, A.C., Cardenas, M.B., Shuai, P., Knappett, P.S., Bennett, P.C., 2016. Groundwater flow, nutrient, and stable isotope dynamics in the parafluvial-hyporheic zone of the regulated Lower Colorado River (Texas, USA) over the course of a small flood. Hydrol. J. 24, 923–935. http://dx.doi.org/10.1007/s10040-016-1365-3.

Cai, Y., Huang, G.H., Nie, X.H., Li, Y.P., Tan, Q., 2007. Municipal solid waste management under uncertainty: a mixed interval parameter fuzzy-stochastic robust programming approach. Environ. Eng. Sci. 24, 338–352. http://dx.doi.org/10.1089/ees.2005.0140.

Cai, Y., Huang, G.H., Yang, Z.F., Sun, W., Chen, B., 2009. Investigation of public's perception towards rural sustainable development based on a two-level expert system. Expert Syst. Appl. 36, 8910–8924. http://dx.doi.org/10.1016/j.eswa.2008.11.032.

Cai, Y., Huang, G.H., Tan, Q., Chen, B., 2011. Identification of optimal strategies for improving eco-resilience to floods in ecologically vulnerable regions of a wetland. Ecol. Modell. 222, 360–369. http://dx.doi.org/10.1016/j.ecolmodel.2009.12.012.

Cardenas, M.B., 2015. Hyporheic zone hydrologic science: a historical account of its emergence and a prospectus. Water Resour. Res. 51, 3601–3616. http://dx.doi.org/10.1002/2015WR017028.

Cheng, L., Li, X., Lin, X., Hou, L., Liu, M., Li, Y., Liu, S., Hu, X., 2016. Dissimilatory nitrate reduction processes in sediments of urban river networks: spatiotemporal variations and environmental implications. Environ. Pollut. 219, 545–554. http://dx.doi.org/10.1016/j.envpol.2016.05.093.

Claret, C., Boulton, A.J., 2009. Integrating hydraulic conductivity with biogeochemical gradients and microbial activity along river–groundwater exchange zones in a subtropical stream. Hydrol. J. 17, 151–160. http://dx.doi.org/10.1007/s10040-008-0373-3.

Cranswick, R.H., Cook, P.G., Lamontagne, S., 2014. Hyporheic zone exchange fluxes and residence times inferred from riverbed temperature and radon data. J. Hydrol. 519, 1870–1881. http://dx.doi.org/10.1016/j.jhydrol.2014.09.059.

Dewes, T., 1996. Effect of pH, temperature, amount of litter and storage density on ammonia emissions from stable manure. J. Agric. Sci. 127, 501–509.

Duff, J.H., Triska, F.J., 2000. Nitrogen Biogeochemistry and Surface-Subsurface Exchange in Streams.

Franken, R.J., Storey, R.G., Dudley Williams, D., 2001. Biological, chemical and physical characteristics of downwelling and upwelling zones in the hyporheic zone of a north-temperate stream. Hydrobiologia 444, 183–195. http://dx.doi.org/10.1023/A:1017598005228.

Gu, C., Anderson, W., Maggi, F., 2012. Riparian biogeochemical hot moments induced by stream fluctuations. Water Resour. Res. 48, w09546. http://dx.doi.org/10.1029/2011WR011720.

Hatch, C.E., Fisher, A.T., Revenaugh, J.S., Constantz, J., Ruehl, C., 2006. Quantifying surface water–groundwater interactions using time series analysis of streambed thermal records: method development. Water Resour. Res. 42, 2405–2411. http://dx.doi.org/10.1029/2005WR004787.

Heppell, C., Heathwaite, A.L., Binley, A., Byrne, P., Ullah, S., Lansdown, K., Keenan, P., Trimmer, M., Zhang, H., 2014. Interpreting spatial patterns in redox and coupled water–nitrogen fluxes in the streambed of a gaining river reach. Biogeochemistry 117, 491–509. http://dx.doi.org/10.1007/s10533-013-9895-4.

Hester, E.T., Hammond, B., Scott, D.T., 2016. Effects of inset floodplains and hyporheic exchange induced by in-stream structures on nitrate removal in a headwater stream. Ecol. Eng. 97, 452–464. http://dx.doi.org/10.1016/j.ecoleng.2016.10.036.

Ingendahl, D., ter Haseborg, E., Meier, M., Van der Most, O., Steele, H., Werner, D., 2002. Linking hyporheic community respiration and inorganic nitrogen transformations in the River Lahn (Germany). Arch. Hydrobiol. 155, 99–120. http://dx.doi.org/10.1127/archiv-hydrobiol/155/2002/99.

Jones, J.B., Holmes, R.M., 1996. Surface-subsurface interactions in stream ecosystems. Trends Ecol. Evol. 11, 239–242. http://dx.doi.org/10.1016/0169-5347(96)10013-6.

Lafrenière, M., Lamoureux, S., 2008. Seasonal dynamics of dissolved nitrogen exports from two High Arctic watersheds, Melville Island, Canada. Hydrol. Res. 39, 323–335. http://dx.doi.org/10.2166/nh.2008.008.

Li, Q., Song, J., Wei, A., Zhang, B., 2013. Changes in major factors affecting the ecosystem health of the Weihe River in Shaanxi Province, China. Front. Environ. Sci. Eng. 7, 875–885. http://dx.doi.org/10.1007/s11783-013-0568-2.

Lin, L., Webster, J.R., Hwang, T., Band, L.E., 2015. Effects of lateral nitrate flux and instream processes on dissolved inorganic nitrogen export in a forested catchment: a model sensitivity analysis. Water Resour. Res. 51, 2680–2695.

Liu, Y., Liu, C., Nelson, W.C., Shi, L., Xu, F., Liu, Y., Yan, A., Zhong, L., Thompson, C., Fredrickson, J.K., 2017. Effect of water chemistry and hydrodynamics on nitrogen transformation activity and microbial community functional potential in hyporheic zone sediment columns. Environ. Sci. Technol. 51, 4877–4886. http://dx.doi.org/10.1021/acs.est.6b05018.

Lowry, C.S., Walker, J.F., Hunt, R.J., Anderson, M.P., 2007. Identifying spatial variability of groundwater discharge in a wetland stream using a distributed temperature sensor. Water Resour. Res. 43, W10408. http://dx.doi.org/10.1029/2007WR006145.

Nowinski, J.D., Cardenas, M.B., Lightbody, A.F., 2011. Evolution of hydraulic conductivity in the floodplain of a meandering river due to hyporheic transport of fine materials. Geophys. Res. Lett. 38, 193–196. http://dx.doi.org/10.1029/2010GL045819.

Rankinen, K., Granlund, K., Etheridge, R., Seuri, P., 2014. Valuation of nitrogen retention as an ecosystem service on a catchment scale. Hydrol. Res. 45, 411–424. http://dx.doi.org/10.2166/nh.2013.239.

Saleem, Z., 1970. A computer method for pumping-test analysis. Groundwater 8, 21–24. http://dx.doi.org/10.1111/j.1745-6584.1970.tb01318.x.

Schullehner, J., Stayner, L., Hansen, B., 2017. Nitrate, nitrite, and ammonium variability in drinking water distribution systems. Int. J. Environ. Res. Public Health 14, 276. http://dx.doi.org/10.3390/ijerph14030276.

Sheibley, R.W., Jackman, A.P., Duff, J.H., Triska, F.J., 2003. Numerical modeling of coupled nitrification–denitrification in sediment perfusion cores from the hyporheic zone of the Shingobee River, MN. Adv. Water Resour. 26, 977–987. http://dx.doi.org/10.1016/S0309-1708(03)00088-5.

Song, J., Chen, X., Cheng, C., Wang, D., Wang, W., 2010. Variability of streambed vertical hydraulic conductivity with depth along the Elkhorn River, Nebraska, USA. Chin. Sci. Bull. 55, 992–999. http://dx.doi.org/10.1007/s11434-009-0640-2.

Song, J., Jiang, W., Xu, S., Zhang, G., Wang, L., Wen, M., Zhang, B., Wang, Y., Long, Y., 2016. Heterogeneity of hydraulic conductivity and Darcian flux in the submerged streambed and adjacent exposed stream bank of the Beiluo River, northwest China. Hydrol. J. 24, 2049–2062. http://dx.doi.org/10.1007/s10040-016-1449-0.

Song, J., Zhang, G., Wang, W., Liu, Q., Jiang, W., Guo, W., Tang, B., Bai, H., Dou, X., 2017. Variability in the vertical hyporheic water exchange effected by hydraulic conductivity and river morphology at a natural confluent meander bend. Hydrol. Processes 31, 3407–3420. http://dx.doi.org/10.1002/hyp.11265.

Stallman, R., 1965. Steady one-dimensional fluid flow in a semi-infinite porous medium with sinusoidal surface temperature. J. Geophys. Res. 70, 2821–2827. http://dx.doi.org/10.1029/JZ070i012p02821.

Stelzer, R.S., Bartsch, L.A., Richardson, W.B., Strauss, E.A., 2011. The dark side of the hyporheic zone: depth profiles of nitrogen and its processing in stream sediments. Freshwater Biol. 56, 2021–2033. http://dx.doi.org/10.1111/j.1365-2427.2011.02632.x.

Stoliker, D.L., Repert, D.A., Smith, R.L., Song, B., LeBlanc, D.R., McCobb, T.D., Conaway, C.H., Hyun, S.P., Koh, D.-C., Moon, H.S., 2016. Hydrologic controls on nitrogen cycling processes and functional gene abundance in sediments of a groundwater flow-through lake. Environ. Sci. Technol. 50, 3649–3657. http://dx.doi.org/10.1021/acs.est.5b06155.

Storey, R.G., Williams, D.D., Fulthorpe, R.R., 2004. Nitrogen processing in the hyporheic zone of a pastoral stream. Biogeochemistry 69, 285–313.

Valett, H.M., Morrice, J.A., Dahm, C.N., Campana, M.E., 1996. Parent lithology, surface–groundwater exchange, and nitrate retention in headwater streams. Limnol. Oceanogr. 41, 333–345. http://dx.doi.org/10.4319/lo.1996.41.2.0333.

Van Raaphorst, W., Malschaert, J.F., 1996. Ammonium adsorption in superficial North Sea sediments. Cont. Shelf Res. 16, 1415–1435. http://dx.doi.org/10.1016/0278-4343(95)00081-X.

Wang, T., Zlotnik, V.A., Wedin, D., Wally, K.D., 2008. Spatial trends in saturated hydraulic conductivity of vegetated dunes in the Nebraska Sand Hills: effects of depth and topography. J. Hydrol. 349, 88–97. http://dx.doi.org/10.1016/j.jhydrol.2007.10.027.

Wang, P., Yu, J., Zhang, Y., Liu, C., 2013. Groundwater recharge and hydrogeochemical evolution in the Ejina Basin, northwest China. J. Hydrol. 476, 72–86. http://dx.doi.org/10.1016/j.jhydrol.2012.10.049.

Wang, S., Lu, A., Dang, S., Chen, F., 2016. Ammonium nitrogen concentration in the Weihe River, central China during 2005–2015. Environ. Earth Sci. 75, 512. http://dx.doi.org/10.1007/s12665-015-5224-7.

Wei, S., Song, J., Khan, N.I., 2012. Simulating and predicting river discharge time series using a wavelet-neural network hybrid modelling approach. Hydrol. Processes 26, 281–296. http://dx.doi.org/10.1002/hyp.8227.

Xu, M.-z., Wang, Z.-y., Pan, B.-z., Na, Z., 2012. Distribution and species composition of macroinvertebrates in the hyporheic zone of bed sediment. Int. J. Sediment Res. 27, 129–140. http://dx.doi.org/10.1016/S1001-6279(12)60022-5.

Xue, Y., Song, J., Zhang, Y., Kong, F., Wen, M., Zhang, G., 2016. Nitrate pollution and preliminary source identification of surface water in a semi-arid river basin, using isotopic and hydrochemical approaches. Water 8, 328. http://dx.doi.org/10.3390/w8080328.

Zachara, J.M., Chen, X., Murray, C., Hammond, G., 2016. River stage influences on uranium transport in a hydrologically dynamic groundwater-surface water transition zone. Water Resour. Res. 52, 1568–1590. http://dx.doi.org/10.1002/2015WR018009.

Zarnetske, J.P., Haggerty, R., Wondzell, S.M., Baker, M.A., 2011. Dynamics of nitrate production and removal as a function of residence time in the hyporheic zone. J. Geophys. Res. Biogeosci. 116, 944–956. http://dx.doi.org/10.1029/2010JG001356. 2011.

Zarnetske, J.P., Haggerty, R., Wondzell, S.M., Bokil, V.A., González-Pinzón, R., 2012. Coupled transport and reaction kinetics control the nitrate source-sink function of hyporheic zones. Water Resour. Res. 48, 299–307. http://dx.doi.org/10.1029/2012WR011894. 2012.

Zhang, Y., Kendy, E., Yu, Q., Liu, C., Shen, Y., Sun, H., 2004. Effect of soil water deficit on evapotranspiration, crop yield, and water use efficiency in the North China Plain. Agric. Water Manage. 64, 107–122. http://dx.doi.org/10.1016/S0378-3774(03)00201-4.

Zhang, Y., Li, F., Zhang, Q., Li, J., Liu, Q., 2014. Tracing nitrate pollution sources and transformation in surface-and ground-waters using environmental isotopes. Sci. Total Environ. 490, 213–222. http://dx.doi.org/10.1016/j.scitotenv.2014.05.004.

Zhang, G., Song, J., Wen, M., Zhang, J., Jiang, W., Wang, L., Kong, F., Wang, Y., 2017. Effect of bank curvatures on hyporheic water exchange at meter scale. Hydrol. Res. 48, 355–369. http://dx.doi.org/10.2166/nh.2016.046.

Zhu, T., Fu, D., Jenkinson, B., Jafvert, C.T., 2015. Calibration and application of an automated seepage meter for monitoring water flow across the sediment-water interface. Environ. Monit. Assess. 187, 171. http://dx.doi.org/10.1007/s10661-015-4388-7.